Crop and Environment 1 (2022) 15–23

Contents lists available at ScienceDirect

Crop and Environment

journal homepage: www.journals.elsevier.com/crop-and-environment

Original Article

Production and scavenging of reactive oxygen species confer to differential sensitivity of rice and wheat to drought stress

Preethi Vijayaraghavareddy [a,b], Sankarapillai V. Lekshmy [a], Paul C. Struik [b], Udayakumar Makarla [a,1], Xinyou Yin [b,*], Sheshshayee Sreeman [a,*]

[a] Department of Crop Physiology, University of Agricultural Sciences, Bengaluru, India
[b] Centre for Crop Systems Analysis, Department of Plant Sciences, Wageningen University & Research, PO Box 430, 6700 AK, Wageningen, the Netherlands

ARTICLE INFO

Keywords:
Drought
Photosynthesis
Reactive oxygen species
Rice
Wheat

ABSTRACT

Drought poses a serious threat to crop production worldwide, and is expected particularly to affect rice production and hence food security. Given that wheat is known to tolerate drought better than rice, we compare rice and wheat (cv. Weebill) to understand the species level differences in drought adaptive mechanisms. We also compare two contrasting rice genotypes (IR64, drought susceptible, and Apo, drought tolerant) for such mechanisms under well-watered (100% field capacity, 100%FC) and water-limited (60%FC) conditions. The reduction in biomass of wheat under water limitation was smaller due to a higher rate of photosynthesis associated with maintenance of tissue turgor compared to rice genotypes. Drought caused greater inhibition of Photosystem II quantum efficiency, carboxylation efficiency, and photosynthetic capacity parameters in IR64 than in Apo. Transcript levels of photosynthesis-related genes were also significantly more repressed by water limitation in IR64, whilst the wheat genotype showed smaller reduction than Apo. Despite higher non-photochemical quenching (NPQ), a smaller increase in scavenging enzymes in IR64 resulted in more accumulation of reactive oxygen species (ROS) in 60%FC than in 100%FC compared to Apo. As a photoprotection mechanism, increased levels of NPQ resulted in lower ROS accumulation in wheat despite the similar increase in scavenging enzyme transcript levels as in Apo, signifying the importance of preventing oxidative burst for enhanced drought tolerance. In Apo, upregulation of the 9-*cis-epoxycarotenoid dioxygenase 2* gene implies the use of xanthophyll pool for the ABA biosynthesis. Our data suggest that regulating photosynthesis and oxidative protection in the wheat genotype enhanced drought tolerance. Improving these traits for rice is crucial to develop drought-tolerant rice genotypes.

1. Introduction

Drought stress induces a series of processes leading to the generation of oxidative stress in plants. Limited availability of water causes the closing of stomata, resulting in the excess of available light energy relative to the available intercellular CO_2. Therefore, the quantity of harvested light energy and generated reducing power can easily surpass the rate of its utilization by the Calvin-Benson-Bassham (CBB) cycle, causing an accumulation of reactive oxygen species (ROS) (Grieco et al., 2020). Overproduction of ROS in various organelles causes oxidative damage to cell components, and activates programmed cell death pathways. The excessive light absorption of stressed plants exacerbates the inactivation of Photosystem II (PSII) under drought (Valladares and Pearcy, 1997). The combination of drought and high light intensity causes oxidative damage to chloroplasts and results in decreased photosynthesis through enhanced production of ROS (Davletova et al., 2005; Niyogi, 1999).

Plants have evolved several photoprotective mechanisms to manage this excess energy, to avoid or minimize cellular damage. These mechanisms include thermal dissipation of light energy, increased photorespiration, and enhanced activity of antioxidant systems under drought conditions (Müller et al., 2005; Šircelj et al., 2007; Wingler et al., 1999). Thermal dissipation of excess energy within the light-harvesting complexes (measured as non-photochemical quenching, NPQ) is believed to be an important and quickly activated regulatory mechanism (Lavaud and Kroth, 2006) involving the xanthophyll cycle (Jahns and Holzwarth, 2012). Increasing NPQ may thus enhance crop performance under stress by reducing cellular damage (Kromdijk et al., 2016). Plants with

* Corresponding authors.
E-mail addresses: xinyou.yin@wur.nl (X. Yin), msshesh1@uasbangalore.edu.in (S. Sreeman).
[1] Deceased on June 26, 2021.

https://doi.org/10.1016/j.crope.2022.03.010
Received 6 October 2021; Received in revised form 26 February 2022; Accepted 28 February 2022

genetically altered NPQ effectively limit photoinhibition (Hubbart et al., 2018; Krah and Logan, 2010).

Antioxidant enzymes and other enzyme-dependent mechanisms control levels of ROS in plant cells. Over the last decades, attempts have been made to improve photoprotection through genetic engineering by manipulating antioxidant enzymes (Ishikawa and Shigeoka, 2008; Nisarga et al., 2017). Apart from activating ROS scavenging mechanisms, avoiding ROS production is equally important. A superior photosynthetic efficiency and/or a higher availability of substrate CO_2 would help consume more electrons and hence can significantly reduce ROS production. Therefore, enhancing carbon uptake by maintaining tissue turgor with an improved photosynthetic machinery is one of the best approaches to reduce ROS production.

Rice (*Oryza sativa* L.) and wheat (*Triticum aestivum* L.) are two C_3 cereals that contribute to over 90% dietary energy requirements of the world. These crops are grown in contrasting environments. While wheat production is predominantly confined to the cool temperature ecosystems, rice is more adapted to tropical climates. These species also differ in their water requirement, with rice requiring much more water than wheat. However, with receding water availability as a result of climate change and competition for water by non-agricultural sectors, there have been serious efforts to explore opportunities of growing rice with less water (Kadam et al., 2015; Ouyang et al., 2017, 2020; Vijayaraghavareddy et al., 2020a). It is envisaged that rice, if grown like wheat in dry soil, will experience much more photo-oxidative stress than wheat because of its semi-aquatic origin. But the narrow genetic variation within species and the difficulty in phenotyping for this trait in a large set of germplasm made it difficult to obtain rice plants with more tolerance to oxidative stress than other dryland cereals. Hence we hypothesised that comparison between species (rice and wheat) may help explore the possible mechanisms to minimize redox burst during drought for crop improvement.

In this study, we used two rice genotypes and one wheat genotype to compare their responses to water limitation. Given that managing oxidative stress either through avoiding production of ROS or effectively scavenging them is known for plants to perform well under stress, our major aim was to compare rice and wheat and ascertain how they differ in their drought stress responses in terms of managing oxidative stress. Apart from gas exchange and ROS measurements, leaf osmotic adjustment, cuticular waxes, and leaf temperature were assessed during the stress period to evaluate the effect of these parameters on drought tolerance and water use efficiency. The comparisons were made between sensitive and tolerant rice genotype and between tolerant rice and wheat genotype. This comparison helps us understand how far the tolerant rice genotype is improved in terms of drought adaptation. It also enhances the knowledge on the complex drought tolerance network in rice and wheat and further aids in narrowing the traits to hasten the selection of genotypes.

2. Materials and methods

Two rice cultivars, IR64 and Apo, and one wheat cultivar, Weebill, were used in this study. Rice genotypes were classified as drought sensitive (IR64, a lowland cultivar with strong reduction in yield under drought) and tolerant (Apo, an aerobic cultivar with small reduction in yield under drought) on the basis of our previous experiment (Vijayaraghavareddy et al., 2020b). Wheat cultivar Weebill is known to be drought tolerant (Ouyang et al., 2017). The experiment was carried out at University of Agricultural Sciences, Bengaluru, India (12°58′N, 77°35′E) during August to October 2017. Experiments were conducted in a controlled greenhouse, set at 22 °C/18 °C day/night temperature and relative humidity of 60% for wheat (average VPD of ~0.5 KPa). For rice, 29 °C/21 °C day/night temperature and 60% relative humidity was maintained (average VPD of ~0.8 KPa). Seeds were planted in containers of 20-L capacity filled with sandy loam soil and farm yard manure in the proportion of 3:1 (w/w). Plants were thinned at 15 days after sowing (DAS) to maintain two plants per pot. Recommended dose of fertilizers ($N–P_2O_5–K_2O$) for rice and wheat was applied in three split doses at 15, 30 and 50 DAS.

2.1. Drought stress imposition and dry matter assessment

A gravimetric method was followed to impose stress. The containers were maintained at 100% field capacity (100%FC) until 30 DAS and stress was introduced thereafter. To impose drought stress, irrigation was withheld to a set of containers. Five biological replicates, i.e. five pots per genotype per treatment, were maintained and pots were arranged in a complete randomised design. It took five days for both rice genotypes and seven days for the wheat genotype to reach 60% field capacity (60% FC) after stress imposition. This level of stress was maintained until the end of the experiment. Soil surface was tightly covered with plastic beads to avoid evaporation. Containers were weighed twice a day between 09:00 to 10:00 h and 15:00 to 16:00 h. Water lost by transpiration was replenished to maintain target field capacity. The experiment was terminated at the booting stage (50 DAS), and plant height and number of tillers were measured before harvesting the plants. Stems, leaves and roots from the plants were separated and oven dried at 60 °C for 3 days. Total dry matter was obtained by summing stem, leaf, and root weights. Total biomass, root weight, root length, leaf area, plant height, and tiller number were measured in five biological replicates. To measure maximum root length, photographs were taken and root volume was measured, also in five replicates. All the other measurements, as described below, were measured in three replicates and samples for these measurements were taken at 40 DAS.

2.2. Osmotic adjustment

The fully expanded second leaves from the top were collected between 10:00 to 10:30 h and were squeezed using a sterile syringe to extract the sap. Osmolality (in mmol L^{-1}) was measured using a vapor pressure osmometer (Vapro, Model 5520, Wescor Inc., Logan, UT, USA). The osmotic potential (MPa) was calculated using:

$$\psi_\pi = -cRT \times 10^{-9}$$

where c is the osmolality (mmol L^{-1} H_2O), R is the universal gas constant (8314 L Pa.K^{-1} mol^{-1}) and T is the temperature (37 °C i.e. 310 K). Difference between the osmotic potential of 100%FC and 60%FC was calculated as the osmotic adjustment (Praba et al., 2009).

2.3. Total chlorophyll content

Chlorophyll content was determined by incubating a known weight of 10 leaf discs from a single plant in 10 mL of acetone (80%):dimethyl sulfoxide (DMSO) (1:1) solution in the dark overnight. The absorbance of each extract was measured at 663 nm and 645 nm using a spectrophotometer. The total chlorophyll content was calculated using the equation given by Arnon (1949) and expressed in mg g^{-1} fresh weight:

$$\text{Chla} = \frac{(12.7 \times \text{A663}) - (2.54 \times \text{A645})}{\text{Weight} \times 1000}$$

$$\text{Chlb} = \frac{(2.54 \times \text{A645}) - (4.68 \times \text{A663})}{\text{Weight} \times 1000}$$

$$\text{Total chlorophyll} = \text{Chla} + \text{Chlb}$$

2.4. Leaf temperature

The leaf temperature was measured using the Fluke thermal imaging system (Fluke Technologies Pvt. Ltd., Everette, Washington, USA). Images were analyzed using SmartView software. The background noise of the image was cleared by outlining the leaf. Data was exported to Microsoft Excel to analyze all the data points of the image (Vijayaraghavareddy et al., 2020a).

2.5. Estimation of cuticular wax content

Cuticular wax content was measured by the colorimetric approach based on the color change generated by the reaction of wax to acidic $K_2Cr_2O_7$ as described by (Mamrutha et al., 2010). A fresh leaf sample (the leaf used for temperature measurements) was immersed into a test tube containing redistilled chloroform (10 mL) for 5 s. Test tubes containing chloroform extract were heated at 75 °C until the smell of chloroform disappeared completely. Later, $K_2Cr_2O_7$ reagent was added and the test tubes were kept at 65 °C for 30 min. Deionized water (12 mL) was added to the test tube after cooling. The absorbance of samples was measured spectrophotometrically at a wavelength of 590 nm. Carnauba wax (Sigma, St. Louis, Missouri, USA) of different concentrations was used to generate a standard graph (Samdur et al., 2003). The total cuticular wax was expressed as μg g^{-1} fresh weight.

2.6. Carbon isotope discrimination ($\Delta^{13}C$)

Stable carbon isotope ratio was measured using an Isotope Ratio Mass Spectrometer (IRMS, DeltaV adv., Thermo Fischer scientific, Bremen, Germany). Dried leaf samples were homogenized into a fine powder which was used for the estimation of carbon isotope composition (Reddy et al., 2020). Sample analysis was done by interfacing the elemental analyser with the IRMS through a continuous flow device (ConFlow III). The isotope composition of the samples was measured along with isotope standards (Potato starch, $\delta^{13}C = -26.85‰$) calibrated against international standards such as ANU sucrose. The carbon isotope composition $\delta^{13}C$ was used in the following equation to obtain carbon isotope discrimination values $\Delta^{13}C$ as proposed by Farquhar et al. (1989) considering the carbon isotope composition of air ($\delta^{13}C_{air}$) as −8.00‰.

$$\Delta^{13}C = \frac{\delta^{13}C_{air} - \delta^{13}C_{sample}}{1 + \delta^{13}C_{sample}/1000}$$

2.7. Superoxide accumulation (O_2^-)

Nitrotetrazolium Blue Chloride (NBT) staining assay in accordance with Vijayaraghavareddy et al. (2020a) was used for the quantification of O_2^- radicals. Excised leaves were immersed into a 0.2% NBT (prepared in 50 mM sodium phosphate buffer, pH = 7.5) and incubated for an hour in darkness. The presence of blue colored compound, formazan, indicates the presence of superoxide. Later, the chlorophyll was removed using a bleaching solution (acetic acid:glycerol:ethanol (1:1:3, v/v/v). Further, to quantify total O_2^- accumulation, the tissues were ground in 0.1% acetic acid supernatant was obtained at 10,000 rpm for 10 min, and absorbance was measured at 560 nm.

2.8. Malondialdehyde content

Malondialdehyde (MDA) as the by-product of lipid peroxidation was extracted from a leaf sample stored at −80 °C using 5 mL of 5% trichloro acetic acid and centrifuged at 12,000 rpm for 15 min. To the extract (1 mL), 2 mL of 0.5% TBA in 20% trichloro acetic acid was added and incubated at 95 °C for 30 min. The reaction was stopped immediately by cooling on an ice bath. Absorbance was recorded at 532 nm and 600 nm and non-specific turbidity was removed by subtracting A600 from A532. Different concentrations of pure MDA (Sigma Aldrich) were used for the standard curve preparation (Nisarga et al., 2017).

2.9. Evans Blue staining

The Evans Blue technique, as described by Vijayaraghavareddy et al. (2017), was used for the quantification of membrane damage. Leaf samples were completely immersed in 5 mL of Evans Blue dye solution prepared by dissolving 0.25 g of dye in 0.1 M $CaCl_2$ (pH 5.6). After incubation for 1 h in darkness, samples were thoroughly rinsed in distilled water to remove unbound dye adhered to the surface. Further, the staining was observed using light microscope (Magnus Analytics, model: MLX).

2.10. Gas exchange and chlorophyll fluorescence measurements

Gas exchange and chlorophyll fluorescence parameters were concurrently measured using a LICOR-6400XT (Lincoln, NE, USA) on the second (counted from the top) fully expanded leaves at 5 days after stress attained at 60%FC. Plants were first dark adapted for 30 min. The *Fo* values were measured under low modulated light over a period of 0.8 s and the *Fm* values were obtained after an application of a 0.8-s pulse of the saturating light (~8000 μmol m^{-2} s^{-1}). Then measurements of response curves started and both the light and CO_2 response curves were measured at 21% oxygen, leaf temperature of 25 °C, and leaf-to-air vapor pressure difference of 1.0–1.6 kPa. The CO_2 response curves were measured at a photosynthetic photon flux density (PPFD) of 1500 μmol m^{-2} s^{-1}, with ambient CO_2 increasing stepwise: 50, 60, 70, 80, 100, 150, 250, 400, 650, 1000, and 1500 μmol mol^{-1}. For light response curves, light intensity was increased stepwise in the order of 30, 50, 70, 100, 200, 500, 1000, 1500, and 2000 μmol m^{-2} s^{-1} while keeping the ambient CO_2 concentration constant at 400 μmol mol^{-1}. At each light or CO_2 step, actinic light intensity (red light) was applied to measure the steady-state chlorophyll fluorescence (*Fs*), and *Fm'* was recorded after applying a 0.8-s pulse of saturating light (~8000 μmol m^{-2} s^{-1}). Apparent quantum yield of PSII electron transport (ϕ_{PSII}) was calculated as: $n_{PSII} = (Fm' - Fs)/Fm'$, and $\Phi PSII = (Fm' - Fs)/Fm'$ NPQ was calculated as: $NPQ = (Fm - Fm')/Fm'$ (Maxwell and Johnson, 2000).

From these measurements (see Supplementary Figs S1 and S2 for the full CO_2- and light-response curves), we derived the following photosynthetic parameters:

- CE, the carboxylation efficiency, which was the linear slope obtained in the initial low part of the curve for assimilation (*A*) against substomatal CO_2 concentration (C_i) (i.e. the part with ambient [CO_2] of 50, 60, 70, 80, and 100 μmol mol^{-1});
- ϕ_{CO2}, quantum efficiency of CO_2 assimilation (on the incident light basis), which was the value of the linear slopes of the initial points of the photosynthetic light response curves (i.e. the part with light intensities of 30, 50, 70, 100, and 200 μmol m^{-2} s^{-1});
- A_{max}, the light saturated (1500 μmol m^{-2} s^{-1}) photosynthetic rate at high CO_2 (1500 μmol mol^{-1});
- A_{sat}, the light saturated (1500 μmol m^{-2} s^{-1}) photosynthetic rate at ambient CO_2 (400 μmol mol^{-1});
- $R_{d,}$ day respiration, estimated as the intercept of the linear regression between photosynthetic rate against $PPFD \cdot \phi_{PSII}/4$ using the initial points of the light response curves (i.e. 30, 50, 70, 100, and 200 μmol m^{-2} s^{-1}) (Yin et al., 2009, 2011).

2.11. RNA extraction

To support the physiological data obtained in this study, a few well-known genes were selected to understand the molecular response of rice and wheat to drought. This included genes related to photochemistry (*psaA, psbA,* and *LHCP2*), biochemistry (*rbcL, rbcS, TPI1*, *FBPase*, and *SBPase*), NPQ (*ZEP* and *VDE*), ABA biosynthesis (*NCED2*) and ROS scavenging (*APX*, *FeSOD*, *CAT*, and *AKR*) (Huang et al., 2021; Zhou et al., 2017). Total RNA was extracted from leaf tissue using the phenol-chloroform method (Datta et al., 1989). A strand of cDNA was synthesized through reverse transcription mediated by M-MLV reverse transcriptase by an oligo (dT) primer and was used as the template for RT-PCR. Quantitative real-time PCR (qRT-PCR) was performed with the fluorescent dye from TAKARA SYBR Green qPCR Kit. The conditions for the PCR amplification were set as follows: one cycle at 94 °C for 3 min, followed by 25 cycles of denaturation at 94 °C for 30 s; 52–58 °C for 30 s; 72 °C for 40 s and 72 °C for 5 min per cycle. The housekeeping ubiquitin gene was used as the reference gene and relative expression of the genes

was estimated using the $2^{-\Delta\Delta CT}$ method. Gene-specific primers were designed using PrimerBLAST software (Ye et al., 2012; also see https://www.ncbi.nlm.nih.gov/tools/primer-blast/).

2.12. Statistical analysis

ANOVA was conducted by using GenStat (15th edition) (http://www.genstat.co.uk/). Least significant difference (LSD) was used to determine the significant difference between genotypes and between treatments.

3. Results

3.1. Effect of drought stress on growth and biomass

Drought during the vegetative stage resulted in a significant reduction in plant height, tiller number, and total leaf area in both rice genotypes with stronger reductions in IR64 than in Apo (Table S1 and Fig. 1a). However, the reduction in all these traits was marginal in wheat genotype Weebill compared with Apo (Fig. 1a). Drought-induced reduction in root weight was significantly higher in the drought-sensitive genotype IR64 than in the drought-tolerant genotype Apo and in the wheat genotype (Fig. 1b). There was no significant change in maximum root length in both species at 60%FC. Between the drought-stress treatments no significant change in root volume and root weight was observed in Apo and Weebill (Fig. 1b). Comparatively, the highest root weight and maximum root length were observed in wheat genotype Weebill followed by Apo in both treatments (Fig. 1b and c and Table S1). Stem and leaf weights were significantly reduced in both species with the strongest reduction in the sensitive genotype IR64 (Fig. 1d). In Apo and Weebill, reduction in stem weight was comparable at ~15% but reduction in leaf weight was higher in Apo than in Weebill. Root to shoot ratio was higher for wheat than for rice (Fig. S3). The reduction in total biomass was higher in IR64 than in Apo and was least in Weebill (Fig. 1d).

3.2. Physiological responses to drought

To assess the effect of drought stress on water relations, osmotic adjustment was measured. Weebill and IR64 showed stronger osmotic adjustment in 60%FC than Apo (Fig. 2a). Relative water content (RWC) of leaves was maintained better in Weebill compared to rice genotypes (Fig. S4). Total chlorophyll content was marginally reduced in IR64 (indicating the degradation of chlorophyll due to stress), while Apo and wheat genotype Weebill showed no marked differences between treatments (Fig. 2b). Since wheat has more glaucous surface compared to rice, cuticular wax content was estimated. Cuticular wax content of Weebill was higher than that of rice genotypes in both 100%FC and 60%FC (Fig. 2c). Of the two rice genotypes, wax load was significantly increased in Apo under drought, whereas IR64 showed no difference between treatments (Fig. 2c). Increase in leaf temperature due to drought stress was lower for Weebill and Apo in both treatments compared to IR64 (Fig. 2d). Carbon isotope discrimination ($\Delta^{13}C$), a proxy for water use efficiency (WUE), was higher in wheat at 100%FC than in rice genotypes (Fig. 2e), suggesting lower WUE in wheat. Whereas, in 60%FC, Apo showed significantly lower $\Delta^{13}C$ than IR64 and Weebill. The percent reduction of $\Delta^{13}C$ at 60%FC was higher in Weebill than in the rice genotypes.

3.3. Accumulation of free radicals and their scavenging

To understand the effect of drought on accumulation of free radicals and their scavenging, ROS and expression of genes associated with scavenging was quantified. Water limitation significantly induced the accumulation of free radicals in both rice and wheat. Of the rice genotypes, IR64 showed higher accumulation of O_2^- and MDA content in 60% FC than Apo and Weebill (Fig. 3a and b). With more free radicals in IR64, significant membrane damage was observed in 60%FC using Evans Blue staining technique. Compared with the rice genotypes, membrane damage was significantly lower in Weebill at 60%FC (Fig. 3c). The expression of scavenging enzymes, ascorbate peroxidase (APX), iron containing superoxide dismutase (FeSOD), catalase (CAT), and aldo-keto reductase (AKR), was significantly upregulated in 60%FC in both species. The fold change in expression at 60%FC over 100%FC was significantly lower in IR64 than in Apo and Weebill, and was not significantly different between Apo and Weebill except for FeSOD (Fig. 3d).

3.4. Effect of drought on photosynthesis parameters

Weebill maintained a higher stomatal conductance than the two rice genotypes under both 100%FC and 60%FC treatments. Of the rice

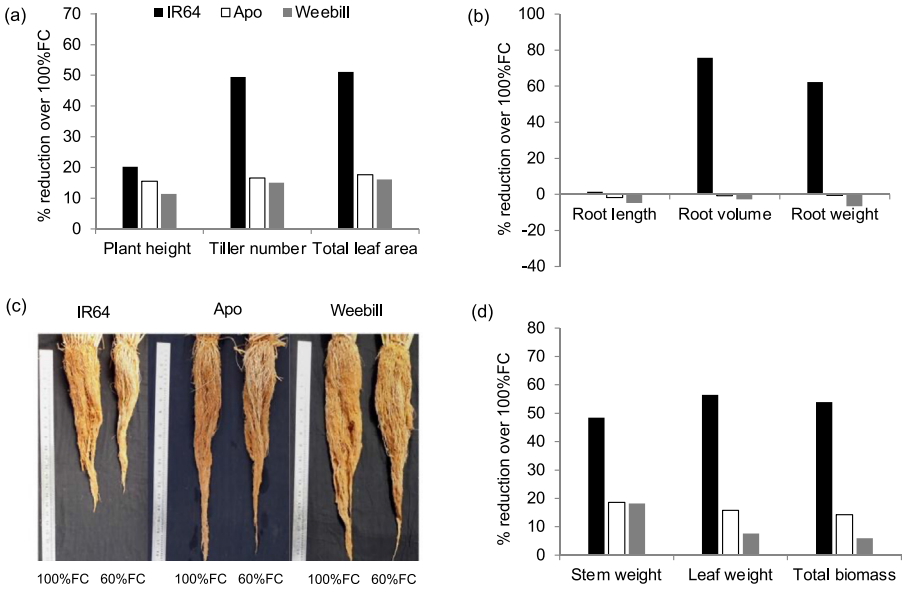

Fig. 1. Effect of drought stress on morpho-physiological parameters of two rice genotypes (IR64 and Apo) and one wheat genotype (Weebill). Percent reduction at 60% field capacity (60%FC) over 100%FC in panel (a) for plant height, tiller number, and total leaf area and in panel (b) for maximum root length, root volume, and root weight; (c) photographs of the root systems of the various genotype × treatment combinations; and (d) the percent reduction at the booting stage in stem weight, leaf weight, and total biomass for plants of 60%FC relative to those of 100% FC. Percent reduction values were calculated from the mean values, which are shown in Table S1.

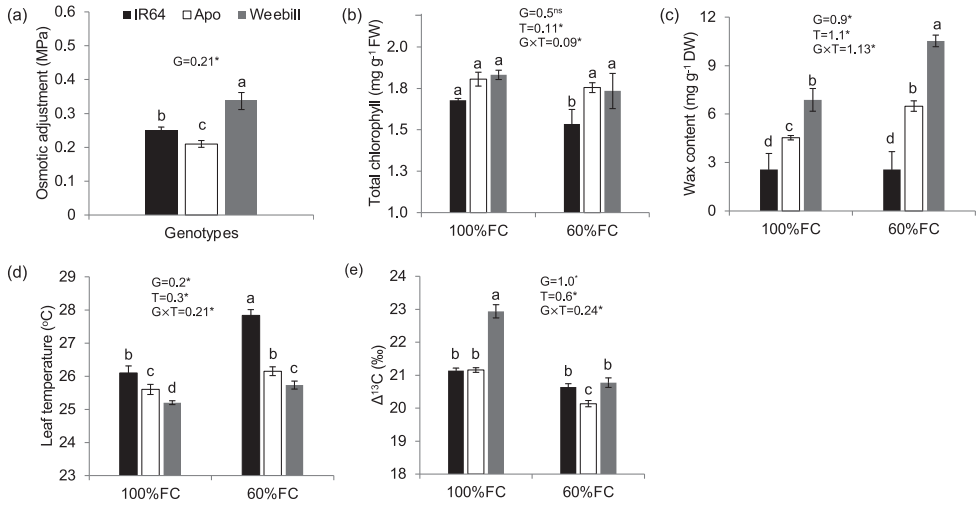

Fig. 2. Effect of drought on physiological parameters of two rice genotypes (IR64 and Apo) and one wheat genotype (Weebill) at 100% field capacity (100%FC) and 60%FC: (a) osmotic adjustment at 60%FC; (b) total chlorophyll content; (c) cuticular wax content; (d) leaf temperature; and (e) carbon isotope discrimination ($\Delta^{13}C$). Error bars indicate the standard error of the mean (mean ± SE). Different letters indicate significant differences ($P < 0.05$) between genotypes from the LSD (least significant difference) post-hoc test determined using one-way ANOVA for osmotic adjustment, or between genotype and treatment combinations from the LSD post-hoc test based on two-way ANOVA for all other parameters. The LSD values are given for genotype (G), treatment (T), and genotype-treatment interaction (G × T).

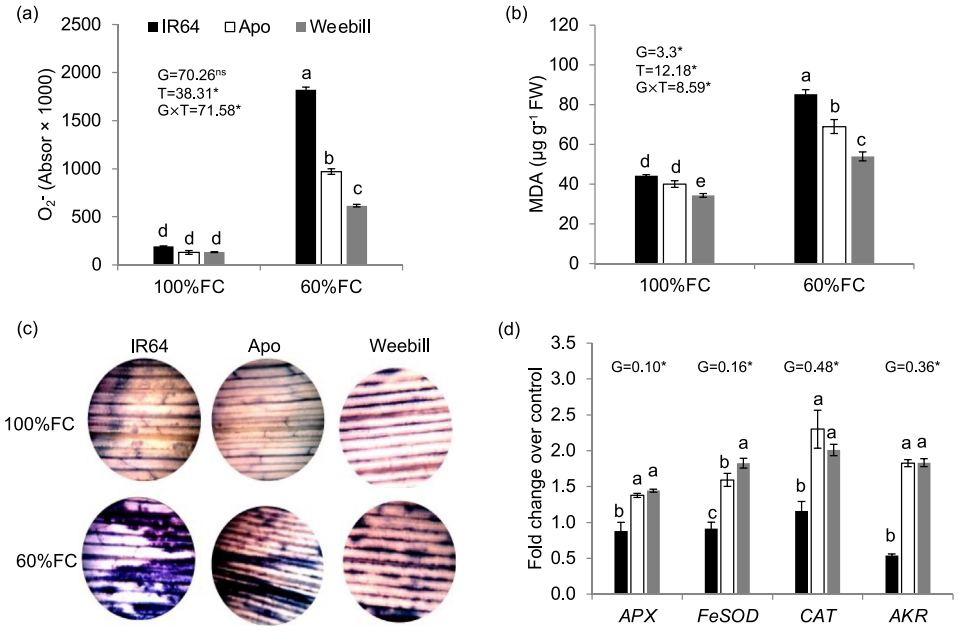

Fig. 3. Effect of drought on ROS accumulation and scavenging in two rice genotypes (IR64 and Apo) and one wheat genotype (Weebill): (a) superoxide (O_2^-); (b) malondialdehyde (MDA) content; (c) photographs of Evans Blue staining; and (d) fold change in expression levels of scavenging enzymes of ascorbate peroxidase (*APX*), iron containing superoxide dismutase (*FeSOD*), catalase (*CAT*), and aldo-keto reductase (*AKR*). Error bars indicate the standard error of the mean (mean ± SE). Different letters indicate significant differences ($P < 0.05$) between genotypes and treatment combinations based on the LSD (least significant difference) post-hoc test determined after a two-way ANOVA for superoxide and MDA content, or between genotypes based on the LSD post-hoc test determined after one-way ANOVA for expression analysis. The LSD values are given for genotype (G), treatment (T), and genotype-treatment interaction (G × T).

genotypes, IR64 showed significantly higher reduction in stomatal conductance in 60%FC compared to a corresponding reduction in Apo (Fig. 4a and Table S2). The light saturated maximum photosynthetic rate under ambient CO_2 (A_{sat}) and that under high CO_2 (A_{max}) conditions were significantly higher for wheat than for the rice genotypes. Of the rice genotypes, reduction in A_{sat} and A_{max} was significantly lower in Apo than in IR64 (Fig. 4b and c and Table S2). Quantum efficiencies of CO_2 assimilation on the incident light basis (ϕ_{CO2}) and carboxylation efficiency (CE) were significantly affected in both species, and comparatively a stronger reduction was noticed in IR64 than in Apo. But wheat maintained significantly higher ϕ_{CO2} and CE in both 100%FC and 60%FC than the rice genotypes (Fig. 4d and e). For day respiration (R_d), IR64 showed a significant increase, Weebill showed a lower increase, but Apo did not show significant increase in 60%FC compared to 100%FC (Fig. 4f and Table S2). Non-photochemical quenching was significantly higher in both rice genotypes at 100%FC compared with the wheat genotype. In 60%FC, although no significant difference was observed within and between species, the percent increase in NPQ was significantly higher for Weebill than for the rice genotypes (Fig. 4g and Table S2). The quantum efficiency of PSII (ϕ_{PSII}) was lower in both species at 60%FC than at 100%FC. Between the species, reduction in ϕ_{PSII} was lower in Weebill and of the rice genotypes, Apo showed lower reduction than IR64 (Fig. 4h and Table S2).

3.5. *Expression of photosynthesis-associated genes*

Expression of a few selected genes was assessed to further understand the effect of drought on photosynthesis. PSI P700 apoprotein A1 (*psaA*), Photosystem II protein D1 (*psbA*), and light harvesting chlorophyll protein 2 *(LHCP2)* gene expression levels were downregulated in 60%FC in rice genotypes with a stronger reduction in IR64 than in Apo (Fig. 5a). Weebill showed a smaller reduction in transcript levels of these genes at 60%FC compared to rice genotypes.

The RuBisCO large subunit (*rbcL*) and small subunit (*rbcS*) gene expression decreased in both rice and wheat by 60%FC (relative to 100% FC), with the strongest reduction noticed in IR64 (Fig. 5b). Transcript levels of triose phosphate isomerase 1 (*TPI1*) were downregulated in both

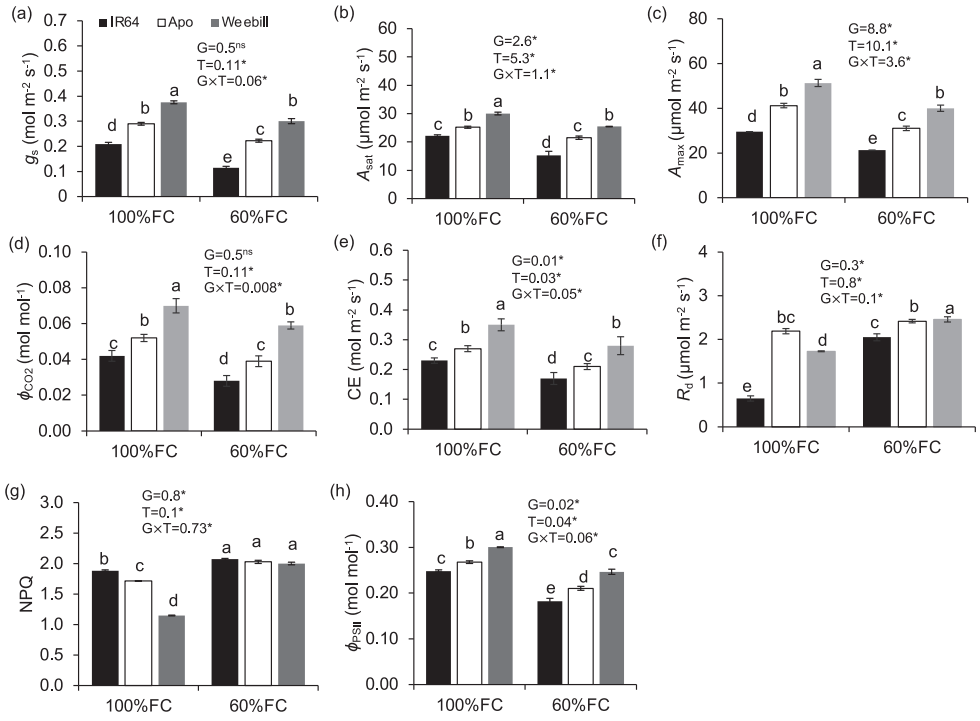

Fig. 4. Effect of drought in two rice genotypes (IR64 and Apo) and one wheat genotype (Weebill): (a) stomatal conductance (g_s) at 1500 μmol m^{-2} s^{-1} of light intensity and ambient [CO_2]; (b) light-saturated maximum photosynthetic rate under ambient [CO_2] (A_{sat}); (c) light-saturated maximum photosynthetic rate at high [CO_2] (A_{max}); (d) quantum efficiency of CO_2 assimilation on the incident light basis (ϕ_{CO2}); (e) carboxylation efficiency (CE); (f) day respiration (R_d); (g) non-photochemical quenching (NPQ) at 1500 μmol m^{-2} s^{-1} of light intensity and ambient [CO_2]; and (h) apparent quantum yield of PSII (ϕ_{PSII}) at 1500 μmol m^{-2} s^{-1} of light intensity and ambient [CO_2]. Error bars indicate the standard error of mean (mean ± SE). Different letters indicate significant difference ($P < 0.05$) between genotype and treatment combinations based on the LSD (least significant difference) post-hoc test after a two-way ANOVA. The LSD values are given for genotype (G), treatment (T), and genotype × treatment interaction (G × T).

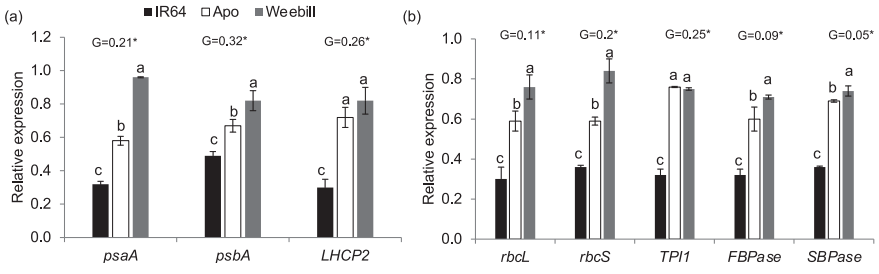

Fig. 5. Effect of drought in two rice genotypes (IR64 and Apo) and one wheat genotype (Weebill) on expression of photosynthetic genes: (a) PSI P700 apoprotein A1 (*psaA*), Photosystem II protein D1 (*psbA*), and light-harvesting chlorophyll-protein 2 (*LHCP2*), and (b) RuBisCO large subunit (*rbcL*) and small subunit (*rbcS*), triose phosphate isomerase 1 (*TPI1*), fructose-1,6-bisphosphatase (*FBPase*) and sedoheptulose-1,7-biphosphatase (*SBPase*). Relative expression was calculated by normalizing the control value to one. Error bars indicate the standard error of the mean (mean ± SE). Different letters indicate significant difference ($P < 0.05$) between genotypes from the LSD (least significant difference) post-hoc test determined using one-way ANOVA. The LSD values are given for genotype (G).

species with higher reduction in IR64 than in Apo. Similar trends were observed for fructose-1,6-bisphosphatase (*FBPase*) and sedoheptulose-1,7-biphosphatase (*SBPase*) transcript levels. Relative expression values of *TPI1*, *FBPase,* and *SBPase* transcripts were similar for Apo and Weebill (Fig. 5b).

3.6. *Expression of xanthophyll cycle and ABA genes*

Since NPQ showed variability among the genotypes, expression analysis was performed for genes associated with the xanthophyll cycle. Expression of *zeaxanthin epoxidase* (*ZEP*) and *violaxanthin de-epoxidase* (*VDE*) genes was upregulated in both species in 60%FC compared with 100%FC. The relative expression level of *ZEP* was significantly higher in Apo, whereas its expression was similar for IR64 and Weebill (Fig. 6a). The relative expression of *VDE* was significantly higher in the wheat genotype compared with both rice genotypes, and was slightly higher in IR64 than in Apo (Fig. 6b). Expression of *9-cis-epoxycarotenoid dioxygenase 2* (*NCED2*), a key abscisic acid (ABA) biosynthetic gene, was measured to notice a significant upregulation in Apo compared with IR64 (Fig. 6c).

4. Discussion

4.1. *Importance of maintaining leaf turgor and cool leaf temperature under drought*

Drought adaptation is strongly linked with sustained carbon metabolism through maintenance of leaf turgor (Sheshshayee et al., 2018). Osmotic adjustment, through accumulation of compatible solutes, is, therefore, one such important mechanism that leads to maintenance of leaf tissue turgor and minimises the harmful effects of drought (Hatzig et al., 2014). In accordance with these reports, our present study revealed that both osmotic adjustment and cuticular wax deposition showed a significant increase under stress (Fig. 2a,c). Our results also showed significant variability existed between and within species and the magnitude of the increase in these mechanisms was more significantly engaged in wheat than in both rice genotypes (Fig. 2). The effect of osmotic adjustment on yield maintenance has been shown in many crops (Morgan, 2000; Santamaria et al., 1990). Additionally, deposition of cuticular waxes plays an important role in drought tolerance (Lokesh et al., 2019). The upregulation of cuticular waxes is greatly influenced by

environmental conditions and the concentration and composition of these waxes vary significantly within and across species (Sánchez et al., 2001). Similarly, increases in cuticular wax load under stress have been observed in wheat and tobacco (Cameron et al., 2006; Elham et al., 2012). These mechanisms might have helped plants maintain a cool canopy and a lower carbon isotope discrimination, resulting in a higher water use efficiency under drought (Impa et al., 2005). Our results suggest that unlike in wheat, upregulating these drought tolerance mechanisms in rice is not sufficient to cope with the water limitation. These results are in agreement with studies in other crop species which showed that enhanced osmotic adjustment and cuticular wax biosynthesis are important to increase drought tolerance by decreasing water use (Cheng et al., 2020; He et al., 2019). Therefore, osmotic adjustment and biosynthesis of cuticular waxes in rice have to be improved to maintain photosynthetic competence under drought.

4.2. Regulation of photosynthesis contributes to drought tolerance

Photosynthesis is one of the primary processes affected by drought, due not only to stomatal closure but also to alterations in the photosynthetic metabolism (Lawlor and Cornic, 2020) and in antenna size and quantum efficiency of PSII (Ha and Papadopoulos, 1999). Water limitation results in downregulation or degradation of RuBisCO and other enzymes of the CBB Cycle, and hence reduces carbon fixation (Feller et al., 2008). In our study, transcript levels of RuBisCO subunits (*rbcs* and *rbcl*), *FBPase*, *SBPase and TPI1* under drought remained stable in wheat compared with rice (Fig. 5b). The initial slope of CO_2 response curves as an indicator of carboxylation efficiency (CE) depends on values of RuBisCO parameters and mesophyll conductance. Photosynthetic rate at ambient CO_2 concentration (A_{sat}) directly reflects the capacity of RuBisCO carboxylation (Lawlor and Cornic, 2002; (Von and Farquhar., 1981). The observations such as CE and A_{sat} (Fig. 4e and f) are consistent with our molecular data. The higher tissue turgor due to osmotic adjustment and cooler canopy in wheat (Fig. 2d and Fig. S3) protects integrity and functionality of the photosynthetic machinery, and therefore, might be responsible for the superior photosynthetic competence of wheat. However, the reason for the superior photosynthetic performance of wheat even under well-watered conditions, compared with both rice genotypes (Fig. 4), needs further analysis.

As a consequence of reduced carbon fixation, the limited utilization of NADPH resulted in overloading of the electron transport chain due to reduced supply of $NADP^+$. This will lead to the formation of ROS via the Mehler reaction (Ramu et al., 2020). In our study, higher rates of D1 protein turnover in wheat (Fig. 5a) provided stability to the photosynthetic electron transport rate from damaging actions of ROS and hence resulted in higher quantum efficiency compared to rice genotypes (Fig. 4d). The increased ROS production causes photoinhibition of PSII and also suppresses the *de novo* synthesis of PSII repair proteins (Aro et al., 2005). But the degree of photoinhibition is highly dependent on the balance between damage to PSII (mainly the D1 and D2 proteins) and activation of the repair process (Nelson and Yocum, 2006; Nishiyama et al., 2006). As a result, many genes associated with photosynthetic pathways will be highly altered to maintain metabolism (Wong et al., 2006). One of the studies reported that a drought-sensitive genotype of barley exhibited a larger decrease in D1 protein content and quantum yield in response to severe drought stress than a tolerant genotype (Ghotbi-Ravandi et al., 2014). Between the rice genotypes, the highest reduction in quantum efficiency of CO_2 assimilation was noticed in IR64 indicating the sensitivity of the genotype to drought (Fig. 4d), and this can trigger the activation of photoprotection mechanisms resulting in competition between thermal dissipation and photochemical reaction (Zhou et al., 2007).

4.3. Increased NPQ in wheat prevents the redox burst

It was always predicted that the level of increase in scavenging mechanisms to detoxify ROS determines the drought tolerance of plants (Lekshmi et al., 2020). But in our earlier study (Vijayaraghavareddy et al., 2020a) as well as in our present study, we observed that the accumulation of ROS in wheat was significantly lower than in the rice genotype Apo despite similar increases in transcript levels of scavenging enzymes (Fig. 3). This could be due to an upregulation of the mechanisms to prevent production of ROS itself, which could be very high in wheat and hence there would be no need to further increase transcript levels of scavenging enzymes. Increasing NPQ is often considered as a rapid feedback response in stress conditions by dissipating excess light energy to prevent further ROS formation (Ballottari et al., 2007). Therefore, NPQ is one of the important mechanisms to avoid ROS hyper accumulation during drought. The increase in NPQ values suggests that the photoprotection mechanism may aid in the stress tolerance in wheat plants by restraining the ROS production but not in rice genotype Apo. The higher ROS accumulation in IR64 (Fig. 3) may be due to stronger photoinhibition and lower transcript levels of scavenging genes compared with genotype Apo. The molecular regulation of NPQ depends on two important genes of the xanthophyll cycle, zeaxanthin epoxidase (*ZEP*) and violoxanthin de-epoxidase (*VDE*) (Jahns et al., 2009). In our study, the increases in NPQ were also evident from the expression of *ZEP* and *VDE*, both being upregulated significantly in wheat and the rice genotypes but the level of upregulation was very distinct in these genotypes (Fig. 6a and b). Suppression of these genes results in lower NPQ levels with higher damage to PSII (Niyogi, 1999). The levels of *VDE* expression will determine the NPQ and ABA accumulation. In wheat and rice genotype IR64, the higher transcript levels of *VDE* resulted in lower ABA biosynthesis, which was evident from lower expression of *NCED2* (Fig. 6c). Comparatively, Apo showed lower *VDE* levels but higher *NCED2* expression (Fig. 6c), indicating utilization of the xanthophyll pool for ABA biosynthesis. The xanthophyll precursor pool also plays an important role in ABA biosynthesis (Zhou et al., 2015). In stress conditions, both *ZEP* and *NCED2* transcript levels will increase to reduce water loss through ABA accumulation (Vijayaraghavareddy et al., 2020b). But the higher expression of *VDE* to regulate the xanthophyll cycle has shown to antagonise the ABA biosynthesis (Zhou et al., 2015). Under aerobic conditions, intermittent drought might trigger ABA biosynthesis as a survival mechanism, however, this hampers the productivity significantly due to stomatal closure (Dharmappa et al., 2019). Hence, screening of germplasm of rice needs to be focused on mechanisms

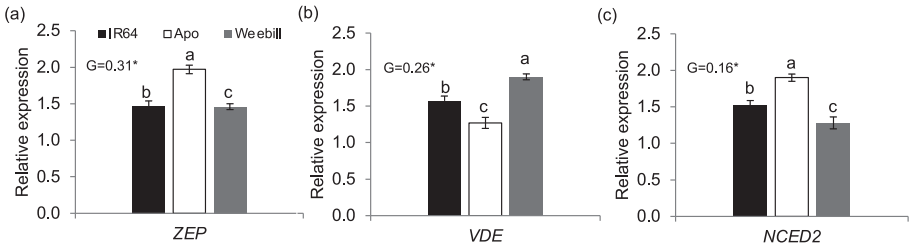

Fig. 6. Effect of drought in two rice genotypes (IR64 and Apo) and one wheat genotype (Weebill) on expression of genes for (a) zeaxanthin epoxidase (*ZEP*), (b) violaxanthin de-epoxidase (*VDE*), and (c) 9-cis-epoxycarotenoid dioxygenase 2 (*NCED2*). Relative expression was calculated by normalizing the control value to one. Error bars indicate the standard error of the mean (mean ± SE). Different letters indicate significant difference ($P < 0.05$) between genotypes from the LSD (least significant difference) post-hoc test determined using one-way ANOVA. The LSD values are given for genotype (G).

associated with preventing ROS production which were lacking in the aerobic rice genotype used in this study.

5. Conclusions

Under drought stress conditions, photosynthesis processes are negatively affected but significant diversity exists in terms of the extent of damage. This study showed that rice and wheat differed in their adaptive mechanisms to drought. The wheat genotype with its stronger adaptive mechanisms to maintain tissue turgor sustained growth under stress with higher WUE and less reduction in carbon assimilation than in both rice genotypes. Within rice, the tolerant genotype Apo showed higher WUE at 60%FC than the sensitive genotype IR64 due to lower leaf temperature and higher accumulation of cuticular waxes. With the maintenance of tissue turgor, both wheat and rice genotype Apo maintained higher photosynthetic capacity and efficiency than IR64. Lower decrease in transcript levels of genes associated with photosynthesis also suggests less damage to photosynthetic machinery in wheat and rice genotype Apo than in IR64. Other than scavenging of ROS, the higher NPQ levels in wheat prevented the ROS formation compared with drought tolerant rice genotype Apo. Although IR64 showed higher NPQ, increased ROS levels due to lower scavenging activity might have resulted in more damage to photosynthetic machinery. Unlike in rice, the maintenance of superior photosynthetic machinery and redox balance in wheat helped sustain growth under stress conditions. Hence, better managing of ROS production is essential for improving rice adaptation to drought.

Declaration of competing interest

The author declares that he/she has no competing interests. Author Xinyou Yin (Editorial Board member) was not involved in the journal's review or decisions related to this manuscript.

Acknowledgements

We thank an anonymous private donor who provided the first author's PhD fellowship and the financial support to this work, *via* Wageningen University Fund. Dr C. G. van der Linden and Dr P. S. Bindraban are acknowledged for their valuable support.

Appendix A. Supplementary data

Supplementary data to this article can be found online at https://doi.org/10.1016/j.crope.2022.03.010

References

Arnon, D.I., 1949. Copper enzymes in isolated chloroplasts. Polyphenoloxidase in Beta vulgaris. Plant Physiol. 24, 1–15.
Aro, E.M., Suorsa, M., Rokka, A., Allahverdiyeva, Y., Paakkarinen, V., Saleem, A., Battchikova, N., Rintamäki, E., 2005. Dynamics of photosystem II: a proteomic approach to thylakoid protein complexes. J. Exp. Bot. 56, 347–356.
Ballottari, M., Dall'Osto, L., Morosinotto, T., Bassi, R., 2007. Contrasting behavior of higher plant photosystem I and II antenna systems during acclimation. J. Biol. Chem. 282, 8947–8958.
Cameron, K.D., Teece, M.A., Smart, L.B., 2006. Increased accumulation of cuticular wax and expression of lipid transfer protein in response to periodic drying events in leaves of tree tobacco. Plant Physiol. 140, 176–183.
Cheng, C., Hu, S., Han, Y., Xia, D., Huang, B.L., Wu, W., Hussain, J., Zhang, X., Huang, B., 2020. Yellow nutsedge WRI4-like gene improves drought tolerance in Arabidopsis thaliana by promoting cuticular wax biosynthesis. BMC Plant Biol. 20, 1–15.
Datta, K., Schmidt, A., Marcus, A., 1989. Characterization of two soybean repetitive proline-rich proteins and a cognate cDNA from germinated axes. Plant Cell 1, 945–952.
Davletova, S., Rizhsky, L., Liang, H., Shengqiang, Z., Oliver, D.J., Coutu, J., Shulaev, V., Schlauch, K., Mittler, R., 2005. Cytosolic ascorbate peroxidase 1 is a central component of the reactive oxygen gene network of Arabidopsis. Plant Cell 17, 268–281.
Dharmappa, P.M., Doddaraju, P., Malagondanahalli, M.V., Rangappa, R.B., Mallikarjuna, N.M., Rajendrareddy, S.H., Ramanjinappa, R., Mavinahalli, R.P., Prasad, T.G., Udayakumar, M., Sheshshayee, S.M., 2019. Introgression of root and water use efficiency traits enhances water productivity: an evidence for physiological breeding in rice (Oryza sativa L.). Rice 12, 1–14.
Elham, F., Khavari-Nejad, R.A., Salekdeh, G.H., Najafi, F., 2012. Evaluation of cuticular wax deposition, stomata and carbohydrate of wheat leaves for screening drought tolerance. Adv. Environ. Biol. 6, 4035–4040.
Farquhar, G.D., Ehleringer, J.R., Hubick, K.T., 1989. Carbon isotope discrimination and photosynthesis. Annu. Rev. Plant Biol. 40, 503–537.
Feller, U., Anders, I., Mae, T., 2008. Rubiscolytics: fate of Rubisco after its enzymatic function in a cell is terminated. J. Exp. Bot. 59, 1615–1624.
Ghotbi-Ravandi, A.A., Shahbazi, M., Shariati, M., Mulo, P., 2014. Effects of mild and severe drought stress on photosynthetic efficiency in tolerant and susceptible barley (*Hordeum vulgare* L.) genotypes. J. Agron. Crop Sci. 200, 403–415.
Grieco, M., Roustan, V., Dermendjiev, G., Rantala, S., Jain, A., Leonardelli, M., Neumann, K., Berger, V., Engelmeier, D., Teige, M., 2020. Adjustment of photosynthetic activity to drought and fluctuating light in wheat. Plant Cell Environ. 43, 1484–1500.
Ha, X., Papadopoulos, A.P., 1999. Effects of supplemental lighting and cover materials on growth, photosynthesis, biomass partitioning, early yield and quality of greenhouse cucumber. Sci. Hortic. 80, 1–18.
Hatzig, S., Zaharia, L.I., Abrams, S., Hohmann, M., Legoahec, L., Bouchereau, A., Nesi, N., Snowdon, R.J., 2014. Early osmotic adjustment responses in drought-resistant and drought-sensitive oilseed rape. J. Integr. Plant Biol. 56, 797–809.
He, J., Jin, Y., Palta, J.A., Liu, H.Y., Chen, Z., Li, F.M., 2019. Exogenous ABA induces osmotic adjustment, improves leaf water relations and water use efficiency, but not yield in soybean under water stress. Agron. 9, 395.
Huang, Y., Huang, Q., Li, J., Yin, Y., Jiao, Z., 2021. Photosynthetic physiology and molecular response mechanisms of indica–japonica intersubspecific tetraploid rice seedlings to ion beams. J. Plant Growth Regul. 40, 722–735.
Hubbart, S., Smillie, I.R., Heatley, M., Swarup, R., Foo, C.C., Zhao, L., Murchie, E.H., 2018. Enhanced thylakoid photoprotection can increase yield and canopy radiation use efficiency in rice. Commun. Biol. 1, 1–12.
Impa, S.M., Nadaradjan, S., Boominathan, P., Shashidhar, G., Bindumadhava, H.Y., Sheshshayee, M.S., 2005. Carbon isotope discrimination accurately reflects variability in WUE measured at a whole plant level in rice. Crop Sci. 45, 2517–2522.
Ishikawa, T., Shigeoka, S., 2008. Recent advances in ascorbate biosynthesis and the physiological significance of ascorbate peroxidase in photosynthesizing organisms. Biosci. Biotechnol. Biochem. 72, 1143–1154.
Jahns, P., Holzwarth, A.R., 2012. The role of the xanthophyll cycle and of lutein in photoprotection of photosystem II. BBA – Bioenergetics 1817, 182–193.
Jahns, P., Latowski, D., Strzalka, K., 2009. Mechanism and regulation of the violaxanthin cycle: the role of antenna proteins and membrane lipids. BBA – Bioenergetics 1787, 3–14.
Kadam, N.N., Yin, X., Bindraban, P.S., Struik, P.C., Jagadish, K.S., 2015. Does morphological and anatomical plasticity during the vegetative stage make wheat more tolerant of water deficit stress than rice? Plant Physiol. 167, 1389–1401.
Krah, N.M., Logan, B.A., 2010. Loss of psbS expression reduces vegetative growth, reproductive output, and light-limited, but not light-saturated, photosynthesis in Arabidopsis thaliana (Brassicaceae) grown in temperate light environments. Am. J. Bot. 97, 644–649.
Kromdijk, J., Głowacka, K., Leonelli, L., Gabilly, S.T., Iwai, M., Niyogi, K.K., 2016. Long, S.P. Improving photosynthesis and crop productivity by accelerating recovery from photoprotection. Science 354, 857–861.
Lavaud, J., Kroth, P.G., 2006. In diatoms, the transthylakoid proton gradient regulates the photoprotective non-photochemical fluorescence quenching beyond its control on the xanthophyll cycle. Plant Cell Physiol. 47, 1010–1016.
Lawlor, D.W., Cornic, G. Photosynthetic carbon assimilation and associated metabolism in relation to water deficits in higher plants. Plant Cell Environ. 25, 275-294.
Leksmi, V.S., Vijayaraghavareddy, P., Nagashree, A.N., Vemanna, R.S., Ramegowda, H.V., Makarla, U., Sreeman, S., 2020. Induction of acquired tolerance through gradual progression of drought is the key for maintenance of spikelet fertility and yield in rice under semi-irrigated aerobic conditions. Front. Plant Sci. 11, 2275.
Lokesh, U., Venkatesh, B., Kiranmai, K., Nareshkumar, N., Amarnathareddy, V., Rao, G.L., Sudhakar, C., 2019. Overexpression of ß-Ketoacyl Co-A Synthase1 gene improves tolerance of drought susceptible groundnut (Arachis hypogaea L.) cultivar K-6 by increased leaf epicuticular wax accumulation. Front. Plant Sci. 9, 1869.
Mamrutha, H.M., Mogili, T., Lakshmi, K.J., Rama, N., Kosma, D., Kumar, M.U., Jenks, M.A., Nataraja, K.N., 2010. Leaf cuticular wax amount and crystal morphology regulate post-harvest water loss in mulberry (Morus species). Plant Physiol. Biochem. 48, 690–696.
Maxwell, K., Johnson, G.N., 2000. Chlorophyll fluorescence–a practical guide. J. Exp. Bot. 51, 659–668.
Morgan, J.M., 2000. Increases in grain yield of wheat by breeding for an osmoregulation gene: relationship to water supply and evaporative demand. Aust. J. Agric. Res. 51, 971–978.
Müller, J., Behrens, T., Diepenbrock, W., 2005. Measurement and modelling of canopy gas exchange of oilseed rape. Agric. For. Meteorol. 132, 181–200.
Nelson, N., Yocum, C.F., 2006. Structure and function of photosystems I and II. Annu. Rev. Plant Biol. 57, 521–565.
Nisarga, K.N., Vemanna, R.S., Chandrashekar, B.K., Rao, H., Vennapusa, A.R., Narasimaha, A., Makarla, U., Basavaiah, M.R., 2017. Aldo-ketoreductase 1 (AKR1) improves seed longevity in tobacco and rice by detoxifying reactive cytotoxic compounds generated during ageing. Rice 10, 1–12.
Nishiyama, Y., Allakhverdiev, S.I., Murata, N., 2006. A new paradigm for the action of reactive oxygen species in the photoinhibition of photosystem II. BBA – Bioenergetics 1757, 742–749.

Niyogi, K.K., 1999. Photoprotection revisited: genetic and molecular approaches. Annu. Rev. Plant Biol. 50, 333–359.
Ouyang, W., Struik, P.C., Yin, X., Yang, J., 2017. Stomatal conductance, mesophyll conductance, and transpiration efficiency in relation to leaf anatomy in rice and wheat genotypes under drought. J. Exp. Bot. 68, 5191–5205.
Ouyang, W., Yin, X., Yang, J., Struik, P.C., 2020. Comparisons with wheat reveal root anatomical and histochemical constraints of rice under water-deficit stress. Plant Soil 452, 547–568.
Praba, M.L., Cairns, J.E., Babu, R.C., Lafitte, H.R., 2009. Identification of physiological traits underlying cultivar differences in drought tolerance in rice and wheat. J. Agron. Crop Sci. 195, 30–46.
Ramu, V.S., Preethi, V., Nisarga, K.N., Srivastava, K.R., Sheshshayee, M.S., Mysore, K.S., Udayakumar, M., 2020. Carbonyl cytotoxicity affects plant cellular processes and detoxifying enzymes scavenge these compounds to improve stress tolerance. J. Agric. Food Chem. 68, 6237–6247.
Reddy, S.H., Singhal, R.K., DaCosta, M.V.J., Kambalimath, S.K., Rajanna, M.P., Muthurajan, R., Sevanthi, A.M., Mohapatra, T., Sarla, N., Chinnusamy, V., Singh, A.K., Sheshshayee, S.M., 2020. Leaf mass area determines water use efficiency through its influence on carbon gain in rice mutants. Physiol. Plantarum 169, 194–213.
Samdur, M.Y., Manivel, P., Jain, V.K., Chikani, B.M., Gor, H.K., Desai, S., Misra, J.B., 2003. Genotypic differences and water-deficit induced enhancement in epicuticular wax load in peanut. Crop Sci. 434, 1294–1299.
Sánchez, F.J., Manzanares, M., de Andrés, E.F., Tenorio, J.L., Ayerbe, L., 2001. Residual transpiration rate, epicuticular wax load and leaf colour of pea plants in drought conditions.19 Influence on harvest index and canopy temperature. Eur. J. Agron. 15, 57–70.
Santamaria, J.M., Ludlow, M.M., Fukai, S., 1990. Contribution of osmotic adjustment to grain yield in Sorghum bicolor (L.) Moench under water-limited conditions. I. Water stress before anthesis. Aust. J. Agric. Research 41, 51–65.
Sheshshayee, S.M., Vijayaraghavareddy, P., Sreevathsa, R., Rajendrareddy, S., Arakesh, S., Bharti, P., Soolanayakanahally, R., 2018. Introgression of physiological traits for a comprehensive improvement of drought adaptation in crop plants. Front. Chem. 6, 92.
Šircelj, H., Tausz, M., Grill, D., Batič, F., 2007. Detecting different levels of drought stress in apple trees (Malus domestica Borkh.) with selected biochemical and physiological parameters. Sci. Hortic. 113, 362–369.
Valladares, F., Pearcy, R.W., 1997. Interactions between water stress, sun-shade acclimation, heat tolerance and photoinhibition in the sclerophyll Heteromeles arbutifolia. Plant Cell Environ. 20, 25–36.
Vijayaraghavareddy, P., Vanitha, A., Ramu, S.V., Sheshshayee, S., Udayakumar, M., 2017. Quantification of membrane damage/cell death using Evan's blue staining technique. Bio-protocol 7, e2519.
Vijayaraghavareddy, P., Vemanna, R.S., Yin, X., Struik, P.C., Makarla, U., Sreeman, S., 2020a. Acquired traits contribute more to drought tolerance in wheat than in rice. Plant Phenomics 5905371.
Vijayaraghavareddy, P., Yin, X., Struik, P.C., Makarla, U., Sreeman, S., 2020b. Responses of lowland, upland and aerobic rice genotypes to water limitation during different phases. Rice Sci. 27, 345–354.
Von, Caemmerer S.V., Farquhar, G.D., 1981. Some relationships between the biochemistry of photosynthesis and the gas exchange of leaves. Planta 153, 376–387.
Wingler, A., Quick, W.P., Bungard, R.A., Bailey, K.J., Lea, P.J., Leegood, R.C., 1999. The role of photorespiration during drought stress: an analysis utilizing barley mutants with reduced activities of photorespiratory enzymes. Plant Cell Environ. 22, 361–373.
Wong, C.C., Li, H.B., Cheng, K.W., Chen, F., 2006. A systematic survey of antioxidant activity of 30 Chinese medicinal plants using the ferric reducing antioxidant power assay. Food Chem. 97, 705–771.
Ye, J., Coulouris, G., Zaretskaya, I., Cutcutache, I., Rozen, S., Madden, T.L., 2012. Primer-BLAST: a tool to design target-specific primers for polymerase chain reaction. BMC Bioinf. 13, 1–11.
Yin, X., Struik, P.C., Romero, P., Harbinson, J., Evers, J.B., Van Der Putten, P.E., Vos, J., 2009. Using combined measurements of gas exchange and chlorophyll fluorescence to estimate parameters of a biochemical C_3 photosynthesis model: a critical appraisal and a new integrated approach applied to leaves in a wheat (Triticum aestivum) canopy. Plant Cell Environ. 32, 448–464.
Yin, X., Sun, Z., Struik, P.C., Gu, J., 2011. Evaluating a new method to estimate the rate of leaf respiration in the light by analysis of combined gas exchange and chlorophyll fluorescence measurements. J. Exp. Bot. 62, 3489–3499.
Zhou, J., Zeng, L., Liu, J., Xing, D., 2015. Manipulation of the xanthophyll cycle increases plant susceptibility to Sclerotinia sclerotiorum. PLoS Pathog. 11, e1004878.
Zhou, K.J., Xia, Wang, Y., Ma, T., Li, Z., 2017. A Young Seedling Stripe2 phenotype in rice is caused by mutation of a chloroplast-localized nucleoside diphosphate kinase 2 required for chloroplast biogenesis. Genet. Mol. Biol. 40, 630–642.
Zhou, Y., Lam, H.M., Zhang, J., 2007. Inhibition of photosynthesis and energy dissipation induced by water and high light stresses in rice. J. Exp. Bot. 58, 1207–1217.